This is the accepted manuscript version of the paper: 10.1109/MetroInd4.0IoT69397.2026.11653173

The final published version is available at: 10.1109/MetroInd4.0IoT69397.2026.11653173

Preliminary Assessment of Printed Strain Gauges for Instrumented Bioreactors

Giona Bonomi, Mauro Serpelloni
Department of Information Engineering
University of Brescia
Brescia, Italy
{giona.bonomi, mauro.serpelloni}@unibs.it

Beatrice Masante, Giovanni Putame, Stefano Gabetti, Diana Massai
Department of Mechanical and Aerospace Engineering
Politecnico di Torino
Torino, Italy
{beatrice.masante, giovanni.putame, stefano.gabetti, diana.massai}@polito.it

***Abstract*—Measurements at small scales are increasingly important in cell-based systems, where controlling and monitoring the culture environment is critical for deriving information related to the cultured construct state. The integration of mechanical sensing into additively manufactured, biocompatible structures represents a novel step toward fully embedded bioreactors. In this work, aerosol jet–printed strain gauges using two silver-based inks (Genesink and UT Dots) were integrated onto four additively manufactured biocompatible samples (BioMed Flex, BioMed Elastic, BioMed Clear, and Surgical Guide) and systematically evaluated. Ink–substrate compatibility tests revealed that highly elastic resins led to cracking and electrical discontinuities, whereas BioMed Clear and Surgical Guide resins ensured continuous conductive traces. Under cyclic tensile loading (0–1 mm), the BioMed Clear-Genesink combination exhibited the highest stability, with a peak drift of only 1.4% of the full-scale range (FSR) and a cycle-to-cycle variation of 0.7% between the 2nd and 20th cycles. In contrast, other configurations showed significantly larger drifts, up to 53.1% in peak variation and over 30% in normalized cycle-to-cycle changes. A cantilever sensing component fabricated with the selected material–ink pair demonstrated repeatable bending detection with a sensitivity of 1.8 Ω/mm in the linear operating region. These results confirm the feasibility of integrating printed strain gauges onto additively manufactured substrates and provide quantitative guidelines for future development of miniaturized mechanical sensing components.**

***Index Terms*—Printed strain gauges, mechanical measurement, bioreactors, biocompatible materials.**

I. Introduction

Over the past two decades, mechanobiology has demonstrated that cells actively sense, transduce, and respond to mechanical cues from their microenvironment, including substrate stiffness, cyclic strain, shear stress, and topographical constraints. Mechanical stimuli represent foundamental regulators of cellular behaviour influencing cell proliferation, differentiation, migration, and gene expression [1] [2]. In stem cell biology, for instance, matrix stiffness alone has been shown to direct lineage specification [3], while dynamic strain modulates cytoskeletal organization and nuclear mechanics [4]. Consequently, the ability to precisely apply and measure mechanical stimuli at small scales becomes an essential feature in the development of advanced systems, such as bioreactors, aimed at providing a controlled and physiologically relevant microenvironment to support cell culture or the formation and maturation in vitro of cell-based constructs, including tissue models.

Several techniques have been developed to quantify cellular and substrate-level mechanical responses. Atomic force microscopy (AFM) enables nanoscale stiffness mapping of cells and tissues [5], while traction force microscopy allows estimation of forces exerted by adherent cells on deformable substrates [6]. However, these techniques are not suitable for a real-time monitoring of the bulk mechanical properties of three dimensional cell-based constructs. Microelectromechanical systems (MEMS)-based sensors have also been used for high-resolution force measurements [7]. Although highly sensitive, these approaches often require complex instrumentation, rigid and/or optically transparent substrates. limiting their integration with bioreactors, especially when additive manufacturing is employed for their prototyping.

Additive manufacturing (AM) has emerged in recent years as an important fabrication technology due to its capability to produce complex three-dimensional structures with high design flexibility. A wide range of material classes are compatible with AM technologies, including photopolymers used in vat-polymerization processes, thermoplastics commonly employed in fused filament fabrication, elastomers, and composite materials. AM is increasingly adopted in biomedical research due to its ability to fabricate complex and patient-specific geometries, using certified biocompatible materials [8] [9]. Indeed, the development of biocompatible materials suitable for additive manufacturing has driven its growing adoption in biomedical research, facilitating the development of innovative custom-made systems, including advanced platforms for cell culture applications [10] [11]. However, while structural components can be readily fabricated, the integration of embedded or surface-mounted mechanical sensors remains a major challenge. Achieving this goal within biocompatible, additively manufactured systems requires sensing technologies that are compatible with polymeric substrates, low-temperature processing, and miniaturized geometries.

Printed electronics provides a promising solution to this integration challenge. Techniques such as inkjet printing, extrusion printing, and aerosol jet printing (AJP) enable the deposition of conductive traces onto flexible and three-dimensional substrates [12]. Among these, AJP offers high resolution and conformal deposition capabilities, making it particularly suitable for non-planar biomedical components [13]. Silver nanoparticle inks are widely used due to their high conductivity and relatively low sintering temperatures [14].

While flexible and stretchable strain sensors have been extensively studied on elastomers such as Polydimethylsiloxane (PDMS) and Thermoplastic Polyurethane (TPU) [15] [16] [17], comparatively little attention has been devoted to the integration of printed strain gauges onto commercially available, biocompatible photopolymer resins used in additive manufacturing. These materials present distinct mechanical behaviors—ranging from rigid to highly elastic—and their compatibility with aerosol jet printed conductive inks has not been systematically assessed. The present study addresses this gap by providing a preliminary but systematic evaluation of aerosol jet printed silver-based strain gauges deposited onto four additively manufactured, biocompatible resin substrates with different mechanical properties. The novelty of this work lies in the combined investigation of (i) ink–substrate morphological compatibility, (ii) electromechanical stability under cyclic tensile loading, and (iii) strain transfer performance in a miniaturized cantilever-like structure. By systematically comparing subtrates of different materials and silver-based inks under realistic loading conditions, this work provides useful operational insights for integrating printed strain sensors into components intended for use as monitoring elements in instrumented bioreactors. Ultimately, the feasibility demonstrated in this study contributes toward the development of bioreactors that can be used for both delivering controlled physical stimulation and monitoring real-time the mechanical properties of cultured cell-based constructs. Such systems represent a critical step toward and quantitative experiments, bridging additive manufacturing, printed electronics, and tissue engineering.

II. Materials and Methods

A. Substrate materials

A total of four materials were selected to investigate suitable substrates for the final structure. Several criteria guided the material selection: the resins were required to be biocompatible, capable of withstanding significant deformation, and compatible with additive manufacturing processes. Based on these requirements, four commercially available resins from FormLabs were selected: BioMed Clear (B-Clear), BioMed Elastic 50A (B-Elastic), BioMed Flex 80A (B-Flex), and Surgical Guide (Surgical).

The main mechanical properties of the selected resins are summarized in Table I. Among the investigated materials, B-Elastic and B-Flex exhibit significantly higher elongation at break (ε_b) compared to B-Clear and Surgical, indicating a markedly more elastic behavior.

TABLE I
Mechanical properties and primary applications of the selected resins

Material	ε_b (%)	σ_b (MPa)	Application
BioMed Clear	12	52	Medical
BioMed Elastic 50A	150	2.3	Medical
BioMed Flex 80A	135	7.2	Medical
Surgical Guide	12	73	Dental

The selected materials were evaluated through three successive experimental steps. In the first step, small rectangular samples were printed and subsequently coated with the conductive ink to assess basic material compatibility and ink adhesion (Fig. 1.a). This preliminary screening aimed to identify potential issues related to ink wetting, adhesion, or curing on the different resin surfaces.

In the second step, dog-bone samples were printed and functionalized with printed strain gauges (Fig. 1.b). These samples were used for tensile tests in order to evaluate the mechanical response of the substrates under deformation and to verify the capability of the strain gauges to detect strain variations. In these first two cases, the geometry of the printed strain sensors follows a typical serpentine layout. In these preliminary experiments, the exact sensor dimensions were not critical, as the objective was primarily to demonstrate the compatibility between the conductive ink and the substrate, as well as the feasibility of strain sensing.

Based on the results of the preceding tests, the final structure was manufactured using the selected material and designed with a cantilever configuration (Fig. 1.c). In this configuration, the beam size was very small (approximately 1 mm), which prevented the use of a conventional serpentine geometry. Because more than two conductive lines could not fit within the beam width, a simplified layout consisting of a single line running up and down was adopted to connect the two contact pads.

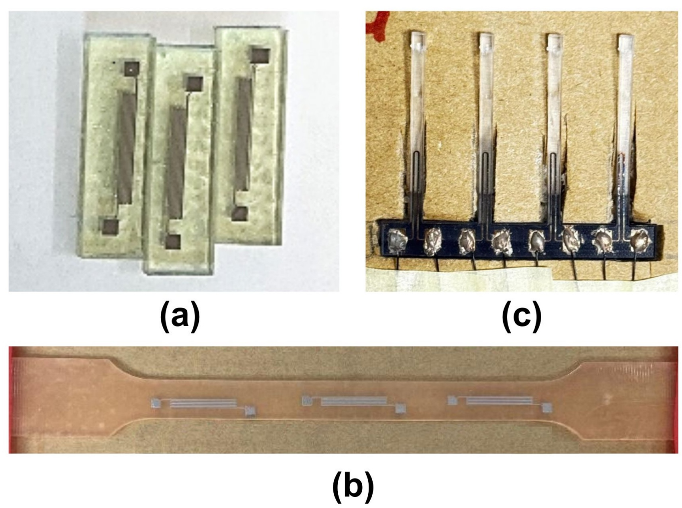

Fig. 1. Printed samples used during the different stages of the experimental campaign: (a) rectangular specimens; (b) dog-bone samples; and (c) final structure integrating four cantilevers in parallel.

B. Printing process

Two silver-based conductive inks were printed using Aerosol Jet Printing (AJP) with an AJ300 system (Optomec, Albuquerque, NM, USA): Smart Aero (Genesink) and

UTDAgPA (UT Dots). The printing parameters for each ink are summarized in Table II. The printing parameters were determined empirically by producing small test patterns and iteratively adjusting the conditions until a stable flow and appropriate ink deposition were achieved, accounting for day-to-day variations in ink viscosity. The two inks required slightly different processing conditions. Genesink required the addition of ethanol in the bubbler, whereas UT Dots was printed without the use of any solvent. In addition, a higher substrate temperature was necessary for the Genesink. Finally, differences in atomizer, sheath, and exhaust pressures were observed between the two inks, reflecting their different viscosities.

TABLE II
AEROSOL JET PRINTING PARAMETERS

Parameter	Genesink	UT Dots
Sheath Flow (sccm)	1000	900
Atomizer Flow (sccm)	612	590
Exhaust Flow (sccm)	550	540
Plate Temperature (°C)	100	60
Number of Passes	3	4
Print Speeds (mm/s)	2-1-1	3-2-1-1
Nozzle Head size (mm)	0.7	0.7

The B-Clear and Surgical substrates were mechanically sanded to remove surface defects and to ensure a uniform printing surface, whereas the B-Elastic and B-Flex substrates were cleaned with ethyl alcohol to remove surface contaminants. After deposition, the printed samples were subjected to a low-temperature thermal treatment at 40 °C.

After drying, the samples were sintered using a photonic sintering process performed with a photonic curing system (PulseForge 1300, Novacentrix, Austin, TX, USA). The processing parameters used for both inks are reported in Table III.

TABLE III
SINTERING PARAMETERS

Parameter	Genesink	UT Dots
Voltage (V)	440	440
Envelope (μs)	3000	3000
μpulses	10	10
Duty Cycle (%)	20	30
Fire Rate (Hz)	0.3	1.3
Repeat Count	10	6

C. Morphological characterization

Morphological characterization was performed using both optical microscopy and profilometric analysis. Optical images were acquired using an NB50T optical microscope (Orma Scientific, Milan, Italy) equipped with a trinocular head and light-emitting diode illumination. This analysis was carried out to assess ink–substrate compatibility and to identify the presence of printing defects.

For a more detailed surface characterization, three-dimensional profilometric measurements were performed using a profilometer (Profilm3D, Filmetrics Headquarters, San Diego, CA, USA).

D. Mechanical Strain Experimental Framework

Both the dog-bone samples and the cantilever prototype were tested to evaluate their performance under mechanical loading conditions using a dynamometer (ESM1500, MARK-10, Copiague, NY, USA). The applied displacement during the tests was measured directly by the dynamometer, while the electrical response of the printed strain gauges was acquired by measuring their resistance with a digital multimeter (KEYSIGHT, Santa Rosa, CA, USA). All instruments were synchronized and controlled using LabVIEW.

The dog-bone samples were clamped vertically between two mechanical grips and subjected to tensile loading. Two different test protocols were applied, both with a maximum displacement of 1 mm and a loading speed of 1.5 mm/min. The gauge length of the specimens was approximately 10 cm; therefore, a maximum displacement of 1 mm corresponds to an applied strain of about 1%. This strain level was selected as a representative small deformation commonly used for the characterization of flexible strain sensors. In the first protocol (called PULL-HOLD or PH), the samples were pulled to 1 mm, held at this displacement for 1 minute, and then released back to 0 mm. This loading cycle was repeated six times to evaluate the stability of the sensor response over time. In the second protocol (PULL-RELEASE or PR), the sample was continuously loaded and unloaded between 0 and 1 mm for 20 consecutive cycles in order to assess the repeatability of the measurements.

For the cantilever prototype, the base of the sample was rigidly clamped, while a vertical displacement was applied at the free tip to induce bending strain in the sensor. The cantilever tip was displaced by 2.5 mm and then released, repeating this up-and-down motion for a total of 10 cycles. The loading speed for these tests was set to 5 mm/min. The chosen displacement corresponds to an estimated maximum surface strain of approximately 0.75% on the beam. This strain level was selected as it represents a moderate deformation expected during operation, while avoiding excessive bending of the cantilever tip that could compromise the structural integrity of the beam, which has a thickness of only 0.8 mm.

III. RESULTS

A. Ink-Substrate Compatibility

All tested materials showed sufficient permeability to allow stable printing. However, cracks were observed in the conductive traces printed on B-Flex and B-Elastic. Profilometer measurements clearly show separations along the conductive paths, which prevent electrical current from flowing (Fig. 2). This issue is caused by the high flexibility of these substrates compared to the inks' compliance. As a result, the printed traces cannot withstand the deformation of the material and break.

In contrast, no damage or interruptions were observed in the traces printed on the other two materials. Both B-Clear and Surgical substrates showed continuous and stable conductive traces with both inks. The main difference between UT Dots

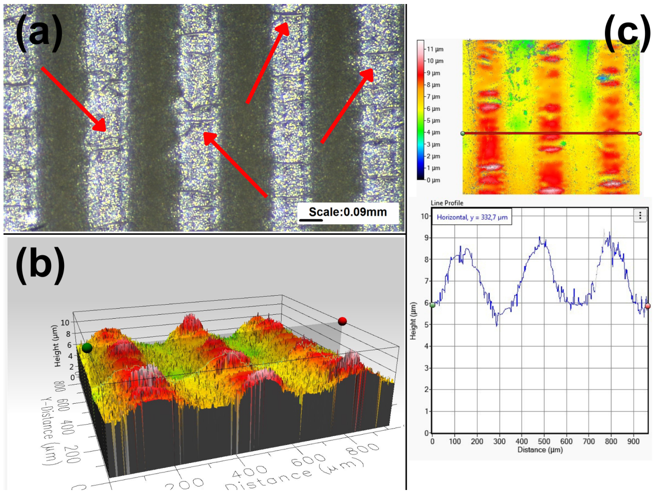

Fig. 2. Genesink's traces on B-Elastic: (a) on microscope with a 0.09 mm scale bar (b) 3D view from profilometer (c) 2D section from profilometer

and Genesink is the shape and height of the printed traces. The first produces higher and sharper profiles, with a trace height of about 8 μm, while Genesink produces smoother and lower traces, with a height of about 5 μm.

Since only the Surgical and B-Clear substrates provided reliable electrical conduction, they were selected for further testing. The B-Flex and B-Elastic substrates were considered incompatible with both inks and were not used in the following experiments.

B. Dog-bone structure

Each dog-bone sample was functionalized with three sensors. The use of multiple sensors allowed verification that the measured resistance values were reproducible and not due to random variations in the printing or measurement process. Among the three printed sensors, only the central one was selected for mechanical testing, as it is located in the region where the deformation field is expected to be more uniform. Table IV reports the mean resistance values along with their corresponding standard deviations for each combination of substrate-ink. Overall, the UT Dots ink exhibits lower resistance values compared to Genesink across the tested substrates. Additionally, for a given ink, the Surgical substrate shows higher resistance values than the B-Clear substrate.

TABLE IV
MEAN AND STD OF SENSORS IN DOG-BONE SPECIMEN AT REST

Substrate-ink	Mean (Ω)	Standard Deviation (Ω)
B-Clear - Genesink,	193.4	±23.3
B-Clear - UT Dots	75.8	±4.9
Surgical - Genesink	354.8	±66.3
Surgical - UT Dots	110	±13.2

All four samples behaved qualitativaley well in both tests being able to detect the strain induced and responding to it. In the PH test, shown in Fig. 3, the samples increase and decrease their resistances in concordance to the stimulus with almost no delay, even though it must be noted that the speed of the test is low so it gives time to respond. All the tests show promising results regarding the stability during the hold phase where the resistance value changed in the worst case of 0.1%, supporting the assumption that during stable phases all the inks and substrates are able to stabilize. If we instead look at the peaks it can be noted that with the sole execption of B-Clear - Genesink all the other samples have a tendency to either increase or decrease their resistance value over time. For reference, the peak values in the B-Clear - Genesink configuration increased by only 1.4% of the full-scale range (FSR), whereas the other Genesink based configuration showed a decrease of 53.1%. In contrast, both UT Dots configurations exhibited an increase in peak value, specifically 31.9% for B-Clear and 14.6% for the Surgical substrate. Since both B-Clear and Surgical exhibited a similar behaviour when printed with UT Dots inks it is likely that the increment in resistance is due to the inks properties. It is possible that, since UT Dots is a less elastic ink than Genesink, this behaviour is the results of cracking of the ink's traces, resulting in an increase in resistance [18]. On the other hand, a similar behavior of the Surgical - Genesink has been reported for other viscoelastic conductive inks, which tend to undergo relaxation phenomena under cyclic loading, leading to a gradual decrease in relative resistance over time [19] [20].

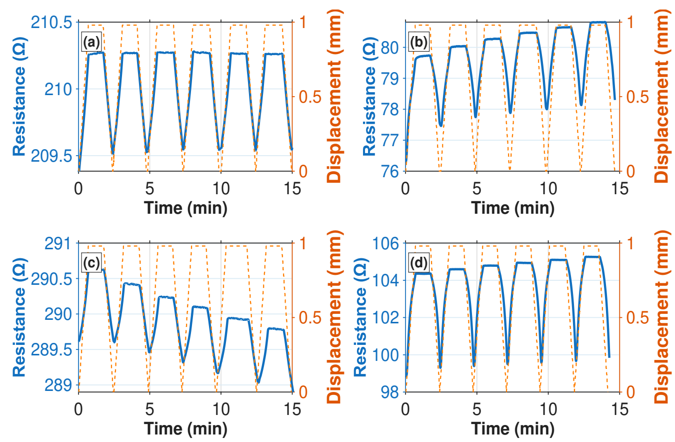

Fig. 3. Samples in the PH protocol of: (a) B-Clear - Genesink, (b) B-Clear - UT Dots, (c) Surgical - Genesink and (d) Surgical - UT Dots

The samples exhibited qualitatively consistent behavior during the PR test (Fig. 4). Table V reports the variation in the initial resistance (R_0) between the 1^{st} and 2^{nd} cycles, and between the 2^{nd} and 20^{th} cycles normalized by the FSR of the smaller of the two corresponding cycles.

TABLE V
CYCLE-TO-CYCLE DRIFT OF INITIAL RESISTANCE

Substrate-ink	1^{st} - 2^{nd} cycle (%)	2^{nd} - 20^{th} cycle (%)
B-Clear - Genesink,	9.6	0.7
B-Clear - UT Dots	13	38
Surgical - Genesink	490	374
Surgical - UT Dots	11.5	22.6

The two substrates functionalized with UT Dots ink exhibited a progressive increase in resistance over time. Although the rate of change decreased with cycling, the variation in resistance between the 2nd and the 20th cycle remained significant, corresponding to 38% of the FSR in one case and 22.6% in the other. A similar trend was observed for the Surgical - Genesink combination, which showed a pronounced decrease in resistance over repeated cycles. This variation was considerably larger than the intrinsic sensitivity of the strain gauge, indicating that the effect cannot be attributed solely to the sensing mechanism. Considering the comparatively high baseline resistance of this sensor with respect to the other substrate printed with the same ink, it is plausible that the sintering process was not fully effective, resulting in a sensing layer with suboptimal electrical and electromechanical performance. In contrast, the B-Clear - Genesink configuration demonstrated the highest stability. After the first loading cycle, the sensor rapidly achieved good repeatability and subsequently exhibited highly consistent responses over successive cycles, with a variation of only 0.7% between the 2nd and the 20th cycle.

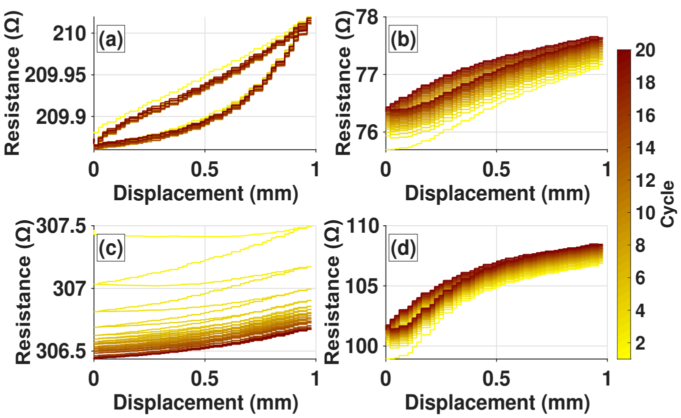

Fig. 4. Samples in the PR protocol of: (a) B-Clear - Genesink, (b) B-Clear - UT Dots, (c) Surgical - Genesink and (d) Surgical - UT Dots

Based on these preliminary results, the combination of material and ink selected for the cantilever prototype was the B-Clear substrate functionalized with Genesink. This choice appears to be the most suitable at this stage, primarily due to its superior stability over time and its rapid attainment of repeatable measurements, requiring only one or two loading cycles.

C. Prototype in cantilever configuration

The cantilever prototype exhibited a reliable mechanical response, demonstrating the ability to detect the deformation applied at the tip through strain measurements at its base. As shown in Fig. 5, the sensor response displayed good repeatability over the first eight loading cycles. A slight decrease in resistance was observed during the last two cycles, which is likely attributable to material relaxation effects previously identified, potentially enhanced by the relatively high strain levels applied to the sensor.

In addition, the signal recorded during the final two cycles appears noisier, suggesting a possible contribution from the electrical wiring. Since the connections used were not flexible, partial mechanical damage or instability during repeated bending cannot be excluded.

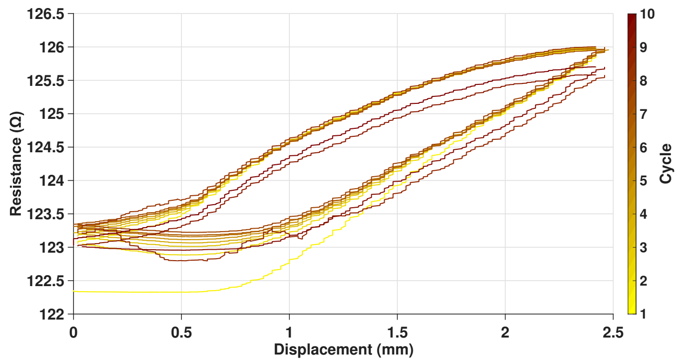

Fig. 5. Bending test of the cantilever at 2.5mm of tip displacement at 5mm/min speed

The sensor response exhibited a nonlinear behavior in the low-displacement regime (0–1 mm), where the sensitivity was significantly lower compared to the higher displacement range between 1 and 2.5 mm. This behavior can be attributed to the presence of a triangular support element positioned beneath the cantilever to enhance structural stability and prevent premature failure. While this reinforcement improves mechanical robustness, it locally increases the stiffness of the structure, thereby limiting strain transfer to the sensor at small displacements ($<$ 1 mm). This limitation can be effectively mitigated by operating the system in a pre-tensioned configuration, ensuring that the sensor primarily functions within the displacement range above 1 mm, where higher sensitivity (of 1.8 Ω/mm) and more linear behavior are observed.

The resistance values of the printed sensors integrated on the cantilever exhibited significant variability, ranging from 61 Ω to 180 Ω, with a mean value of 91 Ω. This spread can be primarily attributed to printing defects and surface irregularities of the substrate. As shown in Fig. 6, the substrate presents randomly distributed defects, and its surface is inherently rough and characterized by pronounced ridges. These imperfections and the lack of surface smoothness affect the uniformity of the printed traces, leading to variations in geometry and, consequently, in the resulting electrical resistance. In future developments, the prototypes will undergo a dedicated surface treatment process aimed at smoothing the substrate and eliminating defects and ridges. This approach is expected to significantly reduce the variability in the printed sensor resistance.

IV. Conclusions and Future Developments

This study presented a preliminary evaluation of aerosol jet printed silver-based strain gauges integrated onto additively manufactured, biocompatible resin substrates for mechanical measurements within bioreactors. The results demonstrate that ink–substrate compatibility strongly depends on the mechanical properties of the underlying material. Highly elastic resins (BioMed Elastic 50A and BioMed Flex 80A) led to

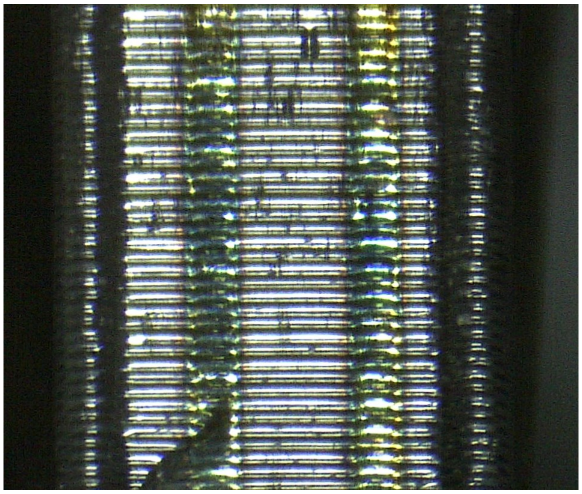

Fig. 6. Imperfections of the prototype's substrate shown at the microscope.

cracking and electrical discontinuities in the conductive traces, indicating insufficient mechanical compliance between ink and substrate. In contrast, BioMed Clear and Surgical Guide substrates ensured stable and continuous conductive paths. Among the tested combinations, BioMed Clear functionalized with Genesink exhibited the most stable and repeatable electromechanical response under cyclic tensile loading. In the PULL-HOLD protocol, this configuration showed a peak drift limited to 1.4% of the full-scale range (FSR), while in the PULL-RELEASE test the cycle-to-cycle variation between the 2^{nd} and 20^{th} cycles was only 0.7%. The cantilever prototype further confirmed the feasibility of integrating printed strain gauges onto additively manufactured components. The selected BioMed Clear-Genesink configuration enabled repeatable bending detection, achieving a sensitivity of 1.8 Ω/mm in the linear operating region (1–2.5 mm displacement). Although nonlinear behavior at low displacement and minor signal drift were observed, the system was able to detect bending-induced strain, providing practical insight into material selection and structural design considerations. Overall, this work establishes the feasibility of using aerosol jet printed strain gauges on biocompatible photopolymer resins and provides initial guidelines for material–ink pairing and mechanical design. While the study does not yet demonstrate biological validation, it defines a technical foundation for instrumented bioreactors enabling real-time monitoring of applied physical stimuli and mechanical characterization of cultured cell-based constructs. Future developments will focus on improving surface finishing to reduce resistance variability, optimizing sintering parameters, and integrating the sensing component into a bioreactor able to provide cyclic stretch stimulation to multiple cell-based constructs.

ACKNOWLEDGMENT

The work is supported by Fondazione Compagnia di San Paolo within the context of the PoC Instrument Linea 1 – PoC Launchpad "Bioreactor integrating an innOvative sensOrised pillars-based frame for electromechanical dynamic STimulation of 3D engineered muscle constructs - BOOST3D.

REFERENCES

[1] D. E. Discher, P. Janmey, and Y. Wang, "Tissue cells feel and respond to the stiffness of their substrate," Science, vol. 310, n. 5751, pp. 1139-1143, Nov 2005.

[2] V. Vogeel, and M. Sheetz, "Local force and geometry sensing regulate cell functions," Nat. Rev. Mol. Cell. Biol., vol. 7, pp. 265-275, Apr 2006.

[3] A. J. Engler, S. Sen, H. L. Sweeney, and D. E. Discher, "Matrix elasticity directs stem cell lineage specification," Cell, vol. 126, pp. 677-689, Aug 2006.

[4] N. Wang, J. D. Tytell, and D. E. Ingber, "Mechanotransduction at a distance: mechanically coupling the extracellular matrix with the nucleus," Nat. Rev. Mol. Cell. Biol., vol. 10, pp. 75-82, Jan 2009.

[5] C. Roduit, S. Sekatski, G. Dietler, S. Catsicas, F. Lafont, and S. Kasas, "Stiffness tomography by atommic force microscopy," Biophysical Journal, v. 97, n. 2, pp. 674-677, Jul 2009.

[6] R. W. Style, R. Boltyanskiy, G. K. German, C. Hyland, et al., "Traction force microscopy in physics and biology," Soft Matter, v. 10, n. 23, pp. 4047–4055, Apr 2014.

[7] J. Rajagopalan, M. T. A. Saif, "MEMS sensors and microsystems for cell mechanobiology,", J. Micromech. Microeng., v. 21, n. 5, 054002, Apr 2011.

[8] A. Wazeer, A. Das, A. Sinha, K. Inaba, S. Ziyi, A. Karmakar, "Additive manufacturing in biomedical field: a critical review on fabrication method, materials used, applications, challenges, and future prospects," Prog. Addit. Manuf., vol. 8, pp. 857–889, Nov. 2022.

[9] M. J. Mirzaali, V. Moosabeiki, S. M. Rajaai, J. Zhou, and A. A. Zadpoor, "Additive manufacturing of biomaterials—design principles and their implementation,", Materials , vol. 15, n. 15, 5457, Aug. 2022.

[10] S. Gabetti, B. Masante, A. Cochis, G. Putame, et al., "An automated 3D-printed perfusion bioreactor combinable with pulsed electromagnetic field stimulators for bone tissue investigations," Sci. Rep., vol. 12, 13859, Aug 2022.

[11] G. Putame, B. Masante, M. Tosini, A. T. Lugas, Ilaria Roato, Mara Terzini, A. L. Audenino, Federico Mussano, and Diana Massai, "A bioreactor-based platform for investigating the early response of human periodontal ligament stem cells to intermittent mechanical stretching," Front. Bioeng. Biotechnol., vol. 13, 1634143 ,Sep 2025.

[12] S. Chandrasekaran, A. Jayakumar, and R. Velu, "A comprehensive review on printed electronics: a technology drift towards a sustainable future," Nanomaterials, vol. 12, n. 23, 4251, Nov 2022.

[13] N. J. Wilkinson1, M. A. A. Smith, R. W. Kay, R. A. Harris, "A review of aerosol jet printing—a non-traditional hybrid process for micro-manufacturing," Int. J. Adv. Manuf. Technol, vol. 105, e4599, May 2019.

[14] C. Y. Lai, C. F. Cheong, J. S. Mandeep, H. B. Abdullah, N. Amin, and K. W. Lai, "Synthesis and characterization of silver nanoparticles and silver inks: review on the past and recent technology roadmaps," J. Mater. Eng. Perform., vol. 23, n. 10, 3541, Oct 2014.

[15] N. A. Vázquez-Torres, J. A. Benítez-Martínez, J. R. Vélez-Cordero, F. M. Sánchez-Arévalo, "Experimental and numerical characterization of a flexible strain sensor based on polydimethylsiloxane polymeric network and MWCNT's," J. Polym. Res., vol. 31, 21, Jul 2024.

[16] W. Muhammad, S. D. Kim, "Highly sensitive and flexible micro-patterned PPy/PDMS strain sensors with enhanced conductivity and stretchability for wearable electronics," Polymer, vol. 308, 127356 ,Aug 2024.

[17] L. Liu, T. Luo, X. Kuang, X. Wan, X. Liang, G. Jiang, H. Cong, and H. He, "Highly stretchable and multimodal MXene/CNTs/TPU flexible resistive sensor with hierarchical structure inspired by annual ring for hand rehabilitation," ACS Sens., vol. 9, n. 5, pp. 2476- 2487, Apr 2024.

[18] Q. Li, A. Antoniou, and O. Pierron, "Understanding resistance increase in composite inks under monotonic and cyclic stretching, " Flex. Print. Electron., vol 7, no. 4, Dec 2022.

[19] S. A. Baker, M. D.McFadden, E. E. Bowden, A. E. Bowden, U. H. Mitchell, and D. T. Fullwood, "Accounting for viscoelasticity when interpreting nano-composite high-deflection strain gauges," Sensors, vol. 22, n. 14, Jul 2022.

[20] Z. Zhang,M. T. Innocent,N. Tang, et al., "Electromechanical performance of strain sensors based on viscoelastic conductive composite polymer fibers," ACS Appl. Mater. Interfaces, vol. 14, n. 39, p. 44832-44840, Sep 2022.